

A Reconfigurable 40 nm CMOS SPAD Array for LiDAR Receiver Validation

Sarrah M. Patanwala^{[1][2]}, Istvan Gyongy^[1], Neale A.W. Dutton^[2], Bruce R. Rae^[2], Robert K. Henderson^[1]

^[1]School of Engineering, Institute for Integrated Micro and Nano Systems, University of Edinburgh, UK, EH9 3FF

^[2]STMicroelectronics Imaging Division, 1 Tanfield, Edinburgh, UK, EH3 5DA

S.Patanwala@ed.ac.uk

Abstract – We present a reconfigurable single photon avalanche diode (SPAD) array realised in 40 nm CMOS technology interfaced to a Xilinx Kintex-7 FPGA, providing the capability to readout 128 channels at 100MHz simultaneously. A Synchronous Summation Technique (SST) to maximise photon detection rate in applications such as automotive LiDAR is proposed demonstrating a 7.5× increase in dynamic range of the system over current state-of-the-art. A simulation model to optimise LiDAR receiver design considering a wide range of parameters is described. Measurements with the test array and a TDC implemented on FPGA are provided to validate the simulations.

I. INTRODUCTION

The ability of Single Photon Avalanche Diodes (SPAD) to provide precise photon arrival times and successful implementations in time-of-flight (ToF) cameras are making them a popular candidate for Light Detection and Ranging (LiDAR) sensors [1][2]. Imaging a scene, for long distance automotive LiDAR applications faces many challenges including scanning a wide field-of-view (FoV), a variety of target reflectivities and harsh ambient conditions. Solid-state LiDAR systems can potentially provide low cost, reliable and compact solutions over current LiDAR systems used for driver assistance and autonomous driving. There are various system parameters, including laser specifications, scanning mechanism, FoV, angular resolution, etc., to be considered for designing a sensor for such systems. Recently, theoretical models have been presented to predict performance for SPAD devices [3][4]. In this paper, we present a test chip to determine the pixel configuration to maximise photon detection rates for the vast dynamic range of signal in the challenging application environment. We also present a simulation model providing LiDAR output in the form of pseudo-realistic histograms. This aims to deliver a thorough comparison platform for evaluating performance and optimal design parameters of a sensor array for different

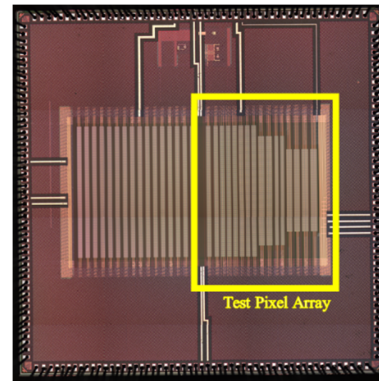


Figure 1 (a): Chip micrograph (highlighted test pixel array)

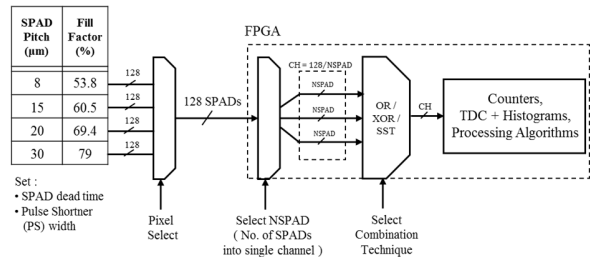


Figure 1 (b): Configuration options available with test chip & FPGA setup

scanning mechanisms and ranging distances under various scenarios.

II. TEST CHIP DESCRIPTION

A reconfigurable SPAD pixel array, realised in STMicroelectronics 40 nm CMOS technology optimised for SPADs [5] is interfaced to a low power, high performance Xilinx Kintex-7 FPGA. Figure 1(a) shows the micrograph of the chip highlighting the test pixel array. SPAD pitch varying from 8μm to 30μm are available, and a maximum number of 128 SPAD digital outputs connected to the FPGA can be read out simultaneously. The number of SPADs and the logic to combine them into a single channel can be selected on the FPGA for required processing. Figure 1(b) shows the available configuration options. This interface provides an ability to record

maximum SPAD events and complete flexibility to evaluate pixel configurations.

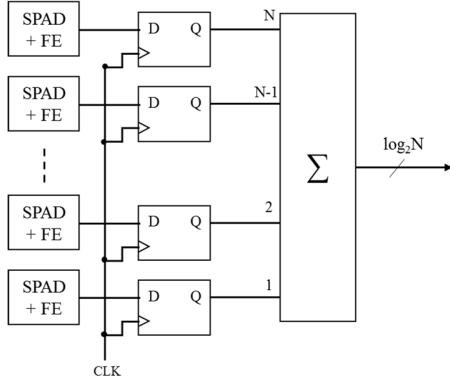


Figure 2 (a): Implementation of SST

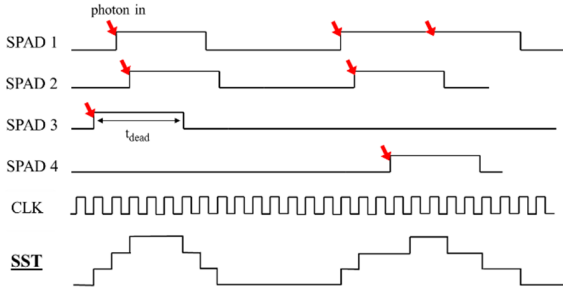


Figure 2 (b): Timing Diagram for SST

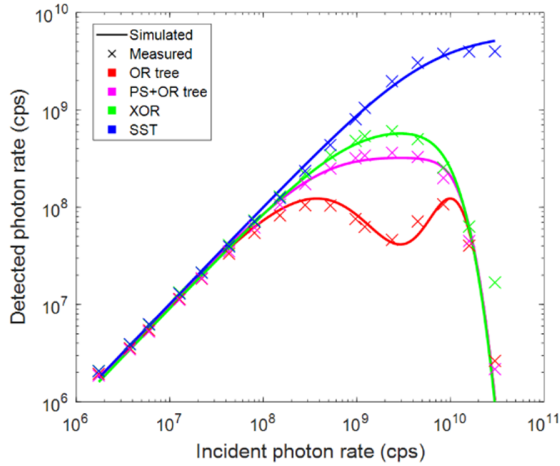


Figure 3: Combining technique count rate analysis—the plot shows the simulated & measured photon count rates through the OR tree, pulse-shortener (PS) with OR tree, XOR tree and SST.

III. COMBINING NETWORK ANALYSIS

In automotive LiDAR applications, a high dynamic range is required to perceive moving objects at unpredictable speeds, at both short and long distances, and subjected to different levels of reflectivity. To

accommodate this high dynamic range, a technique to combine multiple SPAD pulses and increase channel throughput is proposed here, namely the Synchronous Summation Technique (SST). This implementation and timing diagrams are shown in Figure 2. Previously, techniques such as OR tree, a pulse shortener (PS) with OR tree [6] and toggle flop with XOR tree [7] have been reported in literature.

The count rate comparison through OR tree, PS with OR tree, XOR tree and the new SST technique is validated through experimental data and is shown in Figure 3. SST demonstrates an improvement of 30× in dynamic range over OR tree, 15× over PS with OR and 7.5× over XOR tree. It also overcomes the effect of dead-time paralysis of a detector in a channel, which is useful for detecting targets in closer proximity with high reflectivity.

IV. SIMULATED SENSOR PERFORMANCE

A simulation model implemented in MATLAB complements the design of the SPAD test pixel array. It provides an efficient way to model behaviour in terms of photons incident on and detected by the SPADs under a variety of assumptions. The simulator flowchart is shown in Figure 4(a). Initially, system considerations including laser source, optics and scanning mechanism are defined. A vector of time distributed photons incident on the array is generated for the desired scene parameters such as target distance, reflectivity and ambient level. The photon detection algorithm, expanded from [8], processes the stream of incident photons. The algorithm accounts for SPAD parameters such as photon detection probability (PDP), pixel configuration, sensor throughput and biasing conditions, thus accommodating to suit any specific SPAD structures. The output vector of detected photons over given exposures is accumulated to generate histograms and calculate photon detection rates. The programmable parameters in the model are outlined in Figure 4(b). This approach delivers guidelines to maximise detection rate as a function of the design parameters.

The performance of different pixel configurations for the desired ranging is evaluated with parameters such as SPAD pitch, number of SPADs and technique to combine them into a single channel. Effects of detector and channel pile-up [9] and SPAD pitch are prominent factors limiting the maximum imaging distance. For a fixed detector area, SPADs with smaller pitch have less active area resulting in lower photon detection rate. To increase the dynamic range for these smaller SPADs, a higher number of SPADs are

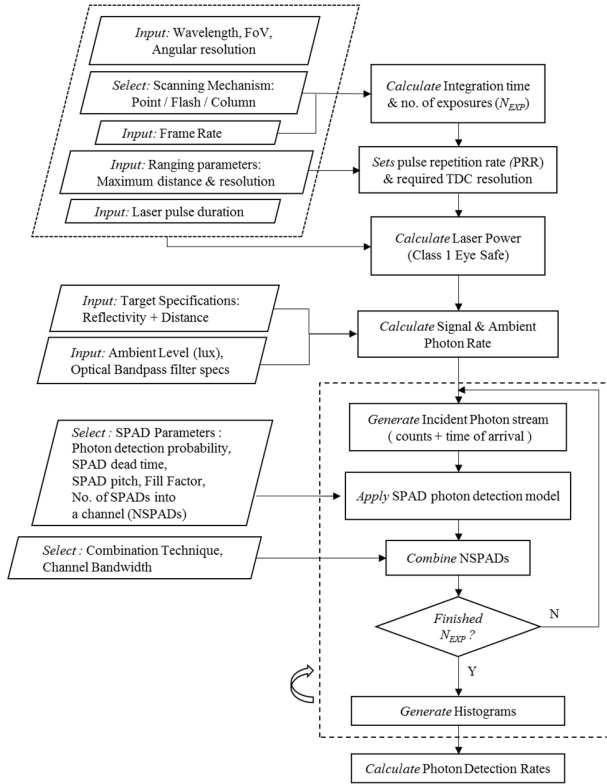


Figure 4 (a): Overview of simulation model flow.

| Design Parameter | | Value |
|--------------------------------|----------------|------------------------------------|
| Wavelength | λ | 905 nm (Fig 4), 840 nm(Fig 5) |
| Field of view | FOV_{XXY} | 120° x 30° |
| Angular Resolution | θ_{XXY} | 0.5° x 0.5° |
| Scanning Mechanism | | Column |
| Frame rate | f_{int} | 30 fps |
| Laser Pulse width | T_{pulse} | 4 ns |
| Laser Power per pixel | P_{pixel} | 15W |
| Pulse repetition rate | PRR | 500 kHz |
| Lambertian target reflectivity | R | 5 – 95% |
| Target distance | d | 0 – 300 m |
| Ambient level | A | 10, 100 klux |
| Optical Bandpass filter | | $(\lambda \pm 25)$ nm |
| Photon detection probability | PDP | 4 % @ 905 nm, 7.2 % @ 840 nm |
| SPAD dead time | t_{dead} | 10 ns |
| Channel bandwidth | f_{BW} | 1 GHz |
| TDC resolution | T_{tdc} | 1 ns |

Figure 4 (b): Design parameters considered for simulation results.

required. However, the performance is then limited by channel pile-up in case of XOR tree. In the case of SST, higher number of SPADs will accommodate more counts at the expense of increased number of read out bits.

A summary of simulated pixel performance is shown, in Figure 5; the figures compare the maximum imaging

distance possible with selected pixel configurations for a range of target reflectivity in ambient level conditions of 10klux and 100klux. The maximum distance is calculated with target detection probability set to 95%, to align with [3], a threshold function of $\sqrt{2\pi \cdot N_{amb}}$ is used, where N_{amb} is the mean value of ambient photons counts.

V. MEASUREMENT RESULTS

The simulation model can be used to generate large sets of histograms for different parameters and evaluate the imaging distance capability of system. To validate these a multiple-event direct histogramming TDC (METDC), based on the approach in [10], was implemented on the FPGA. The TDC has 8 channels in parallel, with a bin resolution of 1ns and 1400 bins, corresponding to range measurements up to 210m with resolution of 15cm. DNL code correction is applied through initial calibration.

The experimental setup consists of a Picoquant pulsed laser with a wavelength of 840nm and pulse width of 6ns FWHM (chosen due to equipment availability). The laser power was scaled with an inverse square law function and delayed through a delay generator to mimic the behaviour of a return signal in a LiDAR environment. A LED with wavelength of 840nm and a measured signal irradiance of 1.3W/m² was used to emulate a constant ambient level. An exposure time of 138 μ s and Pulse Repetition Rate (PRR) of 500kHz was used to match the timing to a column-wise scanning system. The recorded histograms are overlaid and shown in Figure 6. The measurements demonstrate an improved SNR offered by SST, due to its higher photon counting capability. This capability also allows generation of signal content even with low laser return in high ambient level, whereas in the case of XOR tree high ambient photons cause channel pile-up. The inset figures displaying zoomed-in measured and simulated histograms of both methods show a good match.

VI. CONCLUSIONS

A significant improvement in ranging distance is observed by the use of the SST over XOR tree. The simulation model allows synthesising LiDAR outputs and evaluating the required pixel configuration for the desired imaging distance, resulting in an optimised and informed sensor design. The ability to generate validated histogram data in large quantities with known ground truth can enable benchmarking of signal processing algorithms for information extraction without the significant cost and overhead involved in obtaining large amounts of real data.

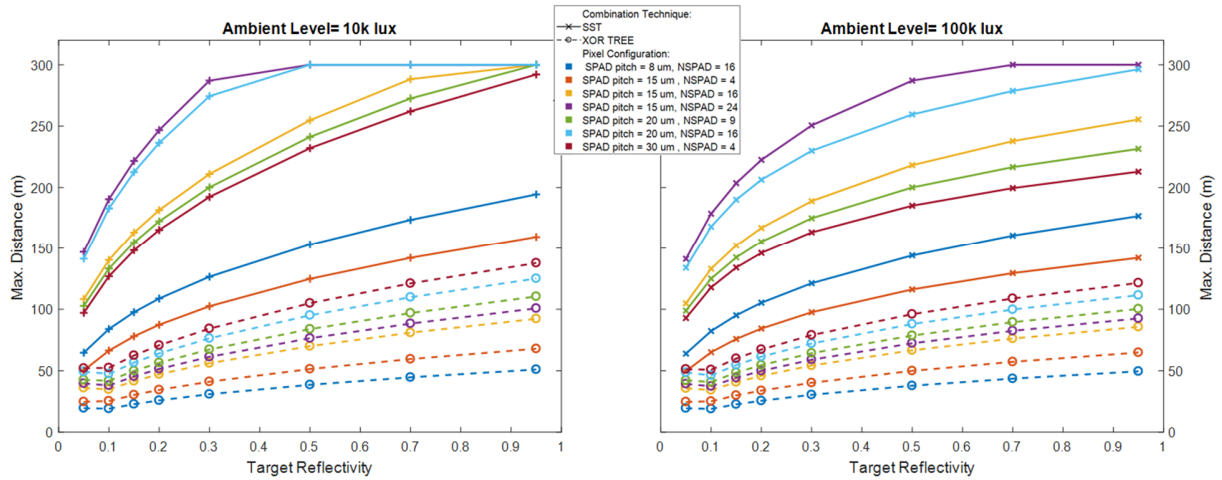


Figure 5 : Simulated Pixel Array performance (includes primary lens) to compare impact of:
 (1) Combining technique: (a) SST (b) XOR tree; (2) SPAD pixel configuration;
 in determining maximum imaging distance for target reflectivity from 5% to 95%.

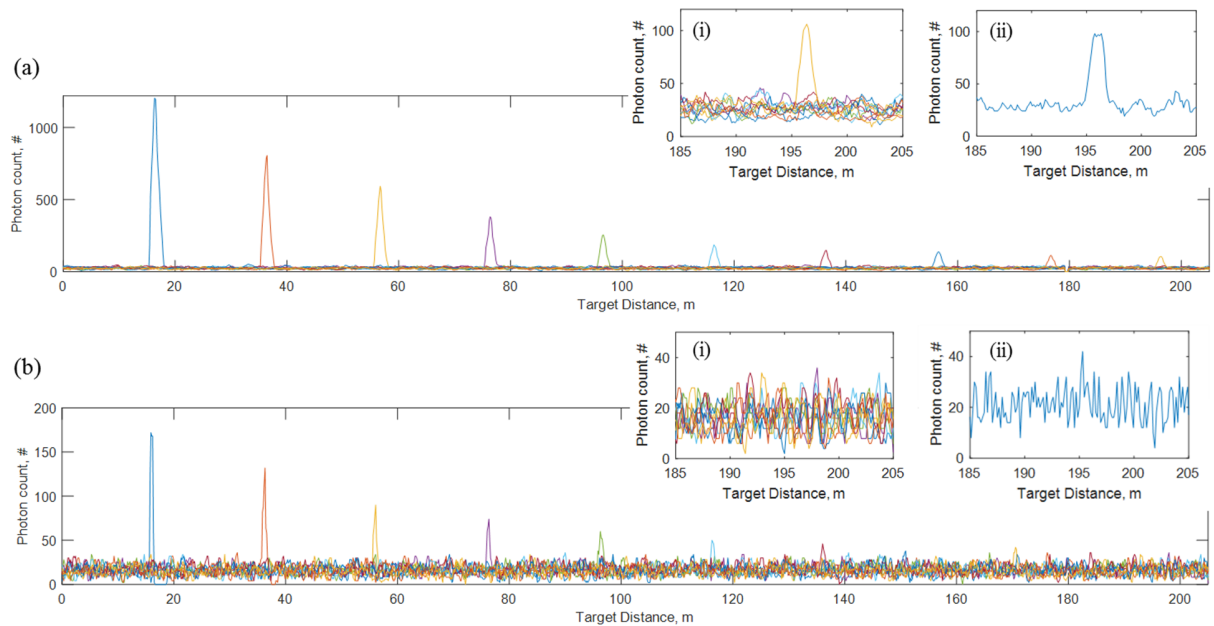


Figure 6 : Histograms measured with FPGA based METDC for Pixel =15 μ m, 24 SPADs,
 Combining technique: (a) SST; (b) XOR Tree. Inset (i) measured, (ii) simulated, results for target 195m.

ACKNOWLEDGEMENTS

We would like to thank Sam Hutchings, Hanning Mai and Francesco M.D. Rocca for helping setup the experiments.

REFERENCES

[1] D. Bronzi, et al., "Automotive Three-Dimensional Vision Through a Single-Photon Counting SPAD Camera", IEEE Transactions on Intelligent Transportation Systems, 2016.
 [2] C. Niclass et al., "A 100-m Range 10-Frame/s 340x96-Pixel Time-of-Flight Depth Sensor in 0.18 μ m CMOS", IEEE JSSC, 2013.

[3] S. Gnechchi and C. Jackson, "A 1x 16 SiPM Array for Automotive 3D Imaging LiDAR Systems". IISW, 2017.
 [4] M. Beer, et al., "Modelling of SPAD-based time-of-flight measurement techniques", Proc. European Conference on Circuit Theory and Design, 2017.
 [5] S. Pellegrini et al., "Industrialised SPAD in 40 nm technology", IEEE IEDM, 2017.
 [6] L. H. C. Braga et al., "A CMOS mini-SiPM detector with in-pixel data compression for PET applications", IEEE Nuclear Science Symp, 2011.
 [7] N. A. W. Dutton, et al., "11.5 A time-correlated single-photon-counting sensor with 14GS/S histogramming time-to-digital converter", ISSCC 2015.
 [8] S. Gnechchi et al., "A Simulation Model for Digital Silicon Photomultipliers", IEEE Transactions on Nuclear Science, 2016.
 [9] J. Arlt, et al., "A study of pile-up in integrated time-correlated single photon counting systems", Rev. Scientific Instruments, 2013.
 [10] N. Dutton et al., "Multiple-event direct to histogram TDC in 65nm FPGA technology," Proc. IEEE PRIME, 2014.